

Accelerated Functional-Level Modeling of More-Electric Aircraft Electrical Power System

S. V. Bozhko, T. Wu, G. M. Asher, and P. W. Wheeler
The University of Nottingham, Nottingham NG7 2RD, United Kingdom
E-mail: serhiy.bozhko@nottingham.ac.uk

Abstract - The more-electric aircraft concept (MEA) is one of the major trends in modern aircraft electric power system (EPS) engineering that results in a significantly increased number of onboard loads driven by power-electronics. Development of appropriate EPS architectures requires intensive simulations to ensure the system integrity, requested quality and performance under possible normal and abnormal scenarios. At the same time, the increased use of tightly-controlled motor drives and power electronic converters can make the simulation of the large-scale EPS impractical due to enormous computation time or numerical non-convergence due to the model complexity. This paper addresses the development of a functional models library capable of significant improvement in simulation time whilst maintaining good accuracy up to a specified frequency range. The library application is demonstrated on the example study of the performance of a twin-generator example EPS under both normal and faulty regimes.

I. INTRODUCTION

The more-electric aircraft (MEA) concept [1] has a significant impact on aircraft power system (EPS) design for next generation airplanes. Many functions that are conventionally managed by hydraulic, pneumatic and mechanical power are replaced by electric power in order to reduce size and weight, and improve fuel efficiency [2]. This will result in wide use of power electronic converters and motor drive systems for such functions as fuel pumping, cabin pressurization and air conditioning, engine start and flight control actuation. Evolution of new EPS architectures evolves in many directions: ac, dc, hybrid, frequency-wild, variable voltage, together with the possibility of novel connectivity topologies. EPS architectures and their attendant power converters will require extensive simulation study, both under operational and fault conditions in order to assess power quality, transient behavior, protection and system availability issues. The new EPS systems are also likely to contain a large number of power electric converters such that a complete representation based on detailed component models will result in very large and perhaps impractical computing times.

To address this issue, a four-layer modeling paradigm has been proposed [3,4] such that each lower layer models the system components to cover successively higher dynamic frequencies. This will be illustrated in details later in a full paper version. The bottom "component" layer aims to a

representative model of each single component behavior, especially for critical components (e.g. solid state switches, electromechanical actuators) covering high frequencies, electromagnetic field and EMC behavior, and perhaps thermal and mechanical stressing. Typically such models are used for verification of local operation and deep analysis of each component behavior. The next level is the "behavioral" layer using lumped parameters subsystem models modeling frequencies up to 100's of kHz and covering converter switching and impact of harmonics and conductive EMC in order to address a network power quality issues. The next level is generally known as the functional layer that addresses steady-state power consumptions and transient behavior (inrush currents, consumption dynamics with regards to input voltage changes etc). Here the power system components are modeled to handle the main system dynamic frequencies of up to $1/3^{\text{rd}}$ of grid frequency (i.e. 100-150Hz) with a time waveform accuracy of 5% in respect of the behavioral model accuracy [4]. The functional level is targeted at power system dynamics, stability, response to loading, and start-up, and aims to model the power system either in its entirety or in sections sufficiently large to obtain a holistic generator-to-load dynamic overview. Finally, the top architectural layer, effectively computes steady state power flow and is used for weight, cost, cabling studies and, most significantly, event modeling and power system reconfiguration studies.

This paper will address the functional modeling for fast computation system studies. It is at this level that the stability and power system control of a chosen architecture is evaluated against the EPS technical and operational specifications. Specific objectives of the functional modeling layer cover the investigation of:

- the system stability and the impact of the EPS control systems (and EPS parameters) on stability margin
- dynamic system performance and EPS quality in response to loading, load dispatching, and regeneration under all flight conditions, as well as EPS start-up operation
- the response to faults, evolution of fault travel in the EPS, isolation and reconfiguration, and fault clearance.

The aim of minimizing computation time whilst maintaining good accuracy up to a given frequency range presents some new modeling challenges, especially as the systems display hard non-linearities so that classical model reduction techniques are not generally applicable. This paper

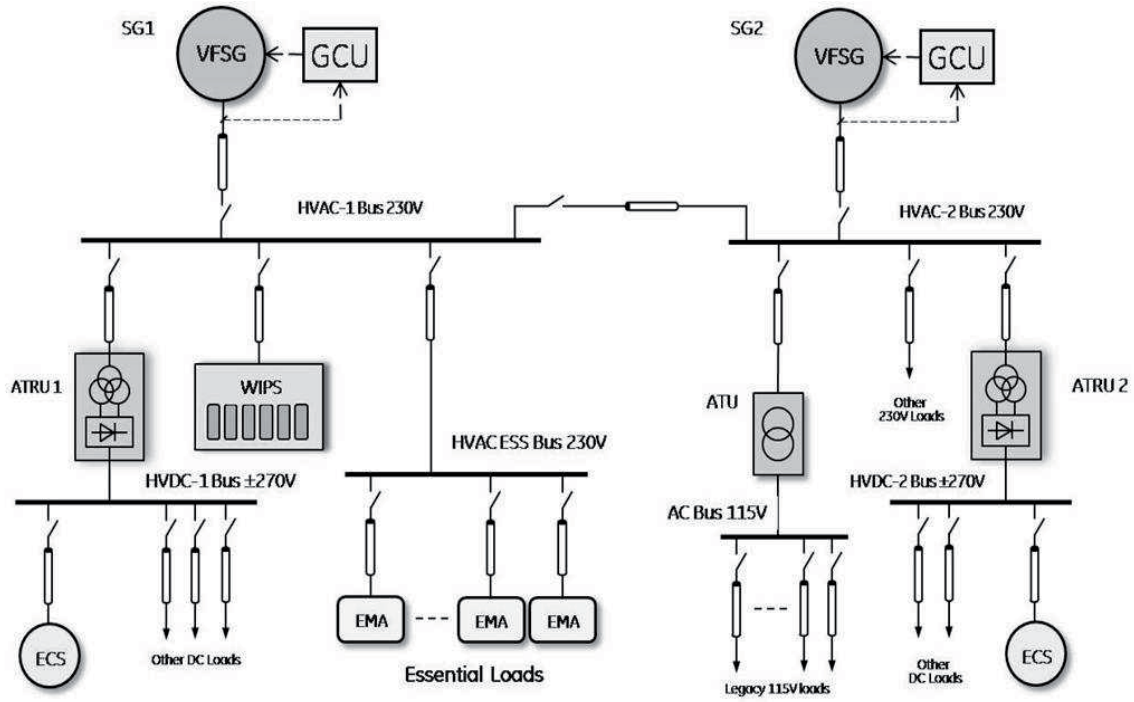


Fig.1. MOET hybrid ac-dc EPS architecture.

will describe the principles upon which the functional models are formulated and will show the significant computational time improvements whilst still meeting good accuracy performance. One aim of the research is to develop a library of functional models that will be common to a large number of architectures; the libraries will be written to operate in the principal software packages like SABER, Modelica or Matlab/Simulink.

The initial library selection covers the modeling of the hybrid ac-dc architecture as defined by MOET large aircraft [4]. A simplification of one half of the EPS is shown in Fig.1 in which only some loads are shown. The EPS is supplied by 2 synchronous generators whose outputs are voltages regulated by a Generator Control Units (GCU). The main buses are a 230V, 360-900Hz frequency-wild. EPS feeds the wing-de-icing WIPS, an essential ac bus HVAC ESS feeding electromechanical actuators through back-to-back PWM converters [5], a 115V ac bus (legacy loads) and a 270V HVDC buses (landing gear, Environmental Control Systems ECS, etc.). The dc buses are fed through nominal 12-pulse autotransformer- rectifier Units (ATRU). Detailed description of the EPS studied will be given in the final manuscript.

A significant issue for the 100-150Hz “low frequency modeling” of ac systems operating at a minimum 300-360Hz frequency is that the steady state ac events are beyond the frequency range of the models. This has led to the view that the ac system need be only represented by phasors representing rms quantities; if the rms quantities vary then this give rise to the term “dynamic phasor” [6]. However, this is misleading since the phase of the steady state waveforms is also required for voltage and reactive power analysis, and

both the magnitude and phase vary within the 150Hz frequency range of interest. As such, this paper will focus on the variable representation of the ac lines as rotating space vectors; this is called the $dq0$ representation. This can produce significant acceleration in computation since the signals are constant in steady state thus presenting a substantially reduced load for the numerical integration algorithms than is the case with ac waveforms to 900Hz.

Line faults and unbalanced operation result in twice frequency variations (ie. 600-1800Hz) and the $dq0$ representation will decelerate as the numerical step lengths reduce to achieve the same error tolerances. Line fault conditions are however of limited duration and the single modeling approach covering un-faulted and faulted conditions without any user intervention is considered very advantageous. The paper includes details on approaches to model all the basic EPS units in $dq0$ domain sand then illustrates few simulation study scenario cases that include typical fault conditions and EPS re-configurations and compare the computation times of both the un-faulted and faulted cases in comparison with a switching benchmark model.

II. FUNCTIONAL MODEL DESCRIPTION

As was already mentioned, the reported models library belongs to the functional modeling level and aims to study events within the 150Hz frequency range using the $dq0$ representation of the ac variables as one of the measures to produce significant acceleration in computation. Since the paper continues our previous studies, details on approaches to model the basic EPS units can be found in the previous

publications. Thus, the details of functional models for the SG and GCU are reported in [7]. The rotor position acts as the $dq0$ frame reference and is available to all other blocks through global memory. The modeling technique for a 12-pulse ATRU unit was reported in our previous work [8] and therefore is not covered here. Basics on actuator modeling are given in [9] where we considered fast functional models for both ac and dc-bus fed EMAs. For the purpose of this study we consider WIPS as a purely resistive load of the appropriate rating. The modeling of EPS fault scenarios was conducted including the effects of mutual coupling and stray capacitance within the cable, as was recently reported in [10]. The technique applied to simulate distribution line faults in the $dq0$ domain using fault-injection block was considered in [7]. In addition, in contrast to the previous reports the interfacing of the functional blocks is now implemented as a 4-wire connection, namely for d , q , 0, and neutral nodes. This allows for the study of unbalanced operation and line-to-line faults in addition to the line-to-ground faults considered in our previous papers

III. MODELING STUDIES OF NON-FAULT CONDITIONS

This section will include results to assess the performance and effectiveness of the functional model of EPS shown in Fig.1 against its benchmark model. Both models were simulated in SABER using Newton-Raphson integration algorithm with standard SABER solver pre-settings. The benchmark model includes full-coil representation of autotransformers with ideal diode bridges and non-switching models for EMA power electronic converters. Due to a limited length of the paper these are not included here but will be reported in the conference presentation. In the figures shown and discussed below, simulation results from both benchmark and functional models are overlaid upon each other.

To perform the simulation comparison, both EPS models were “powered-up” to the rated voltages (230Vrms at HVAC’s at 400Hz, 540V at HVDC’s and 800Vdc in

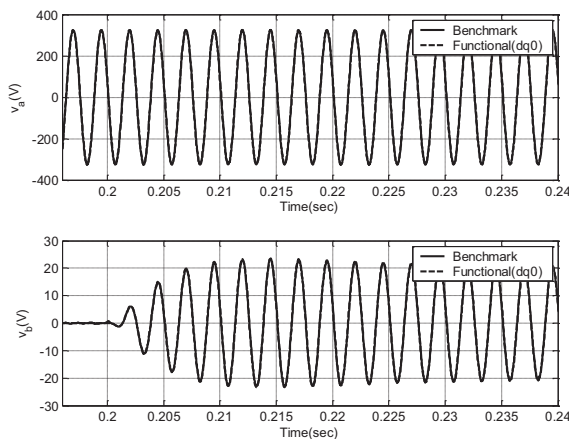


Fig. 2. The dynamic response of the VHVAC and i_{cru} to a step change in EMA power demand

actuators dc links. The first experiment simulates step change of EMA power demand from 0 to 10kW at $t=0.2s$. Figure 2 depicts the response of HVAC bus voltage (namely, phase A) and current drawn by EMA (for the phase A as well) from the HVAC ESS bus. In addition, Fig.3 shows EMA dc-link voltage and current responses.

As it follows from the results above, there is a very good match between the benchmark and the functional EPS models. This confirms that the proposed functional modeling approach is capable of accurate modeling of both the steady state and the normal transient behavior of the aircraft EPS.

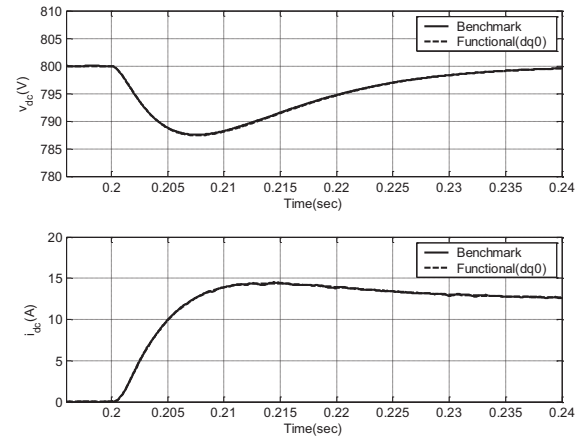


Fig. 3. The dynamic response of the $v_{dc,cru}$ and $i_{dc,cru}$ to a step change in EMA power demand.

Effectiveness of the functional modeling approach can be judged by comparing the computation time taken by the benchmark and the functional models in simulating 1-second of a steady state EPS operation. Both the models were simulated in SABER with the Newton-Raphson integration algorithm with the variable time step. The computation taken is shown in Table 1 for different truncation error settings. For the benchmark model, good simulation results can be obtained if the truncation error is set to 0.001% or less. In the mean time, the functional model delivers good matching results (as shown in Figures 2 and 3) if the truncation error setting relieved to 0.1%. Thus, the acceleration in computation can be evaluated as $111/0.264 \approx 420$. So, the functional domain modeling allows for a significant acceleration in simulation of steady-state EPS operation.

TABLE 1 COMPUTATION TIME TAKEN FOR SIMULATION OF 1S STEADY-STATE EPS OPERATION

Truncation error	Benchmark Model (s)	Functional Model (s)
0.1%	34.5	0.264
0.01%	58.1	0.328
0.001%	111	0.391
0.0001%	380	0.458

IV. MODELING STUDIES OF FAULT CONDITIONS

This section will demonstrate the performance and effectiveness of the functional model against its benchmark model under EPS faulty operation.

For the aircraft EPS it is of great importance to study the dynamic response during possible abnormal conditions. This section will demonstrate the application of the developed functional models library within a simulation study of the example twin-generator EPS during the following fault scenarios:

- loss of one generator (SG1);
- short-circuit fault at HVDC-1;
- line-to-line fault in the cable feeding ATRU1.

The simulation results of these three scenarios are reported below.

Loss of one generator (SG1)

It is assumed that a fault occurs internally in the SG1 resulting in its disconnection from HVAC-1. The fault is detected in 10ms and the control logic closes inter-bus switch to feed HVAC-1 from SG2. In order to assess the impact of SG1 loss on the EPS behavior under the worst-case scenario, all ECSs, EMAs and other loads are assumed to be under full power conditions. In order to avoid SG2 overloading, the WIPS, according to the event logic, is forced to go into a stand-by mode with only 1kW of power consumed to maintain the temperature of the aircraft wing. For the same purpose, all the HVAC2 ac loads are also disconnected.

Results from the benchmark and functional models are given below. In Fig.4 the disconnection of SG1 occurs at $t=1.2$ s with subsequent reconfiguration to SG2 after 10ms. Due to the control action of GCU2, the voltage at the now “common” HVAC bus (bottom window in Fig.4) recovers to the rated value of 230Vrms, and the quality of the transient can be assessed against different standards or requirements of the installed equipment.

The impact of the reconfiguration on the motor drive loads within the EPS system is a crucial consideration within

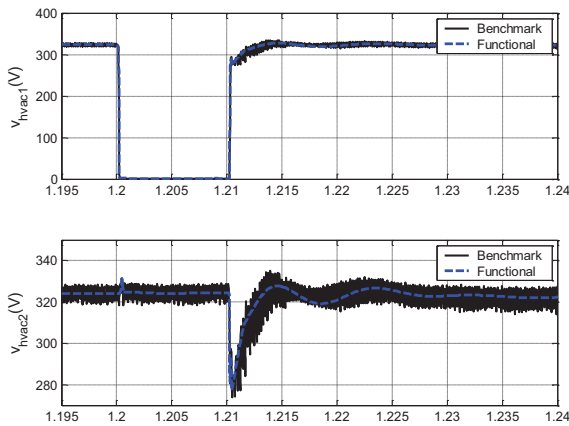


Fig.4. Transient response of v_{HVAC1} and v_{HVAC2} on SG1 loss

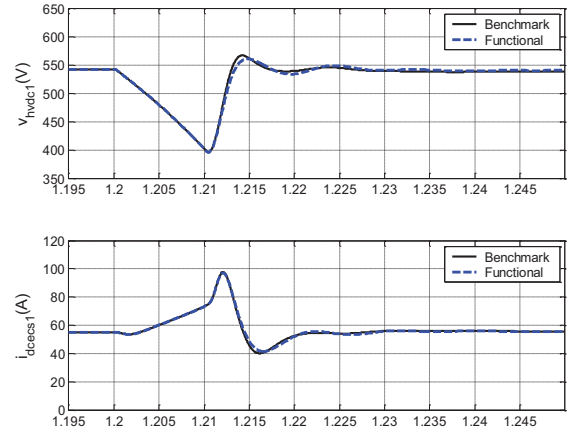


Fig.5. The dynamic response of v_{HVDC1} and i_{dcECS1} to the SG1 loss

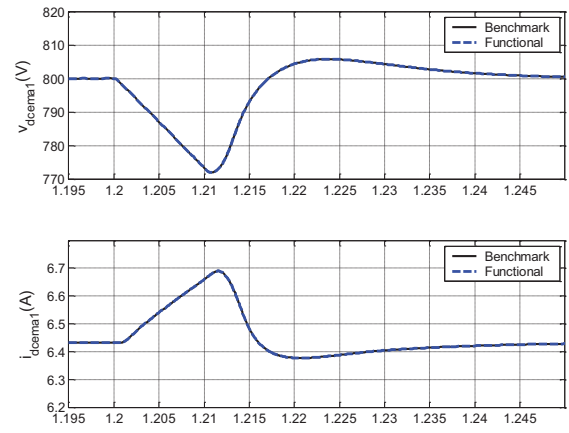


Fig.6. The response of v_{dcEMA1} and i_{dcEMA1} to a loss of SG1

aircraft systems. Figure 5 shows the dynamic response of HVDC-1 voltage v_{HVDC1} and ECS-1 current i_{dcECS1} to the loss of SG1 while Fig.6 shows the response of EMA dc-link voltage and current.

Although v_{HVAC1} is interrupted due to the loss of SG1, the ECS and EMAs during reconfiguration draw current from their dc-link capacitors. This results in a drop of corresponding dc-link voltages (here, v_{HVDC1} and v_{dcEMA1}) with subsequent recovery due to the action of corresponding controls. If during the reconfiguration the dc-link voltage in some of the active loads drops below the threshold of under-voltage protection, the corresponding EMA or ECS will be tripped-out. In the case studied the voltage drop occurring at, for example, HVDC1 does not cause the ECS1 to stop ensuring safe environmental conditions onboard during the studied events. Similar can be concluded for EMA – the actuator will not trip-out during the studied scenario.

Many other interactions within the EPS can be studied as well, depending of the simulation purpose. Fig.7, for example, shows the effect of the generators switchover on the HVDC-2 voltage and current drawn by ECS fed from this bus.

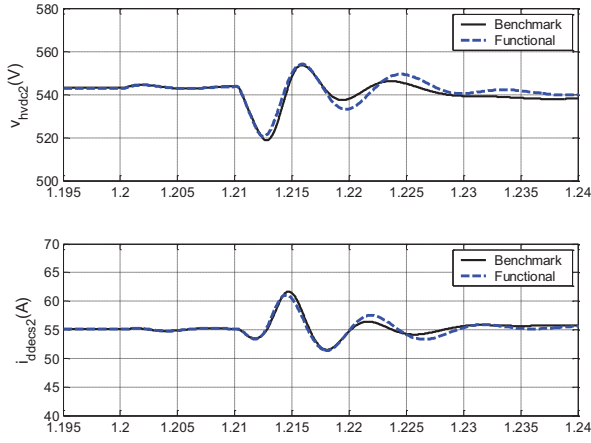


Fig.7. The response of HVDC2 voltage and ECS2 current on SG1 loss

Short-circuit fault at HVDC1

This Section reports the simulation study results for the event of a short-circuit fault occurring on the HVDC1 bus. The fault was simulated by a sudden impact of tiny resistance on one of the dc feeders at $t=1.3$ s with subsequent disconnection of the faulty circuit in 10ms. Figure 8 shows the transient response of the HVAC1 voltage, ATRU1 current and HVDC1 voltage during the scenario.

Fig. 9 depicts the impact of the HVDC1 fault on the AC ESS bus feeding flight critical equipment. As can be observed, the effect on the EMAs during the studied scenario will be small due to the fast clearance action and due to the internal controls capable of maintaining the corresponding dc-link voltages for the duration of fault.

Line-to-line fault in the cable feeding ATRU1

In this Section we demonstrate the capabilities of the proposed models to handle unbalanced line-fault conditions by the simulation of a line-to-line fault occurring on the cable feeding ATRU1. If such a fault occurs, it can be cleared by disconnection of the faulty circuit. As a result, ATRU1 together with HVDC1 and all associated loads including ECS1 will be lost. In the simulations below we assume the fault occurs at $t=1.4$ s and is cleared in 10ms at $t=1.41$ s. During these 10ms the HVAC1 voltage will exhibit an unbalanced three-phase system with harmonics due to the negative sequence current component, as the simulation results in Fig.10 show. Note that the results are shown in the ordinary abc terms reconstructed from calculations in the $dq0$ domain for illustrative purposes.

Fig. 11 shows the response HVDC1 voltage v_{HVDC1} and ATRU1 output current $i_{dc,atru1}$. The drop of v_{HVDC1} at the initial fault stage is because the $i_{dc,atru1}$ becomes zero and the dc-link capacitor is discharged. When the v_{HVDC1} drops to a certain level, the inrush current $i_{dc,atru1}$ will charge the dc-link capacitor immediately. In steady state, the reduction of v_{HVAC1} causes the reduction of v_{HVDC1} . Since ECS1 acts as a constant-power load, the averaged $i_{dc,atru1}$ value will adversely increase

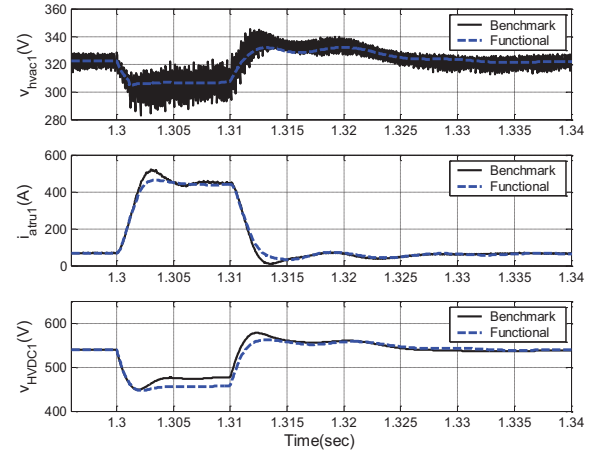


Fig.8. The response of HVAC1 voltage, ATRU1 current and HVDC1 voltage to a short-circuit fault on HVDC1 bus

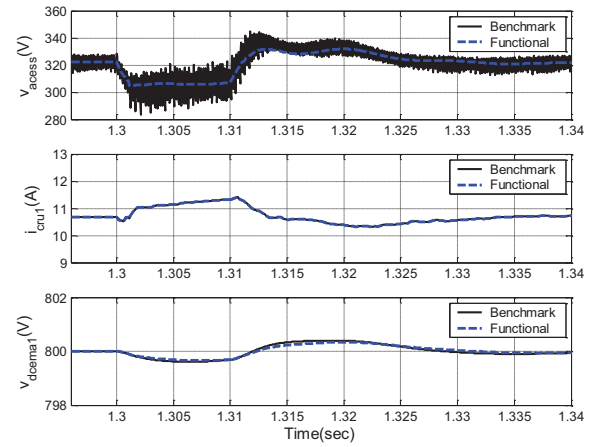


Fig.9. The response of HVAC ESS bus voltage, EMA current and EMA dc-link voltage to a short-circuit fault on HVDC1

until v_{HVDC1} drops to its steady-state value. The $i_{dc,atru1}$ becomes discontinuous causing a significant ripple in v_{HVDC1} . When the fault clears, three-phase i_{atru1} becomes zero since the ATRU1 is disconnected and v_{HVDC1} drops until it hits the ECS undervoltage protection threshold.

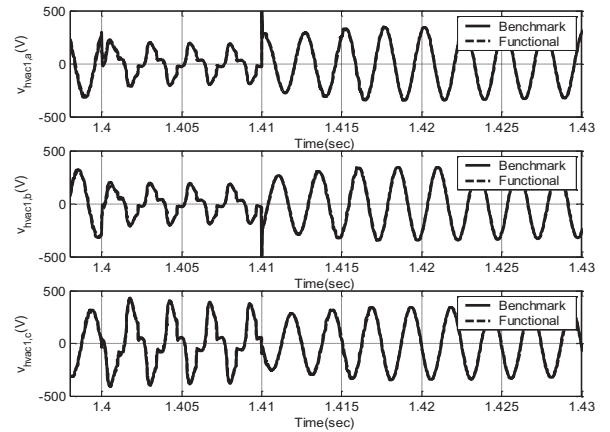


Fig.10. The HVAC-1 response to a line-to-line fault (abc voltages)

V. CONCLUSIONS

This paper reports the development of a functional models library that can be used for accelerated simulation studies of complex more-electric aircraft EPS architectures. The capabilities of the developed library were illustrated by a simulation study of two-generator EPS under both normal and faulty operation. The proposed accelerated modeling approach provides an efficient and accurate tool for system engineers to design and optimize a variety of aircraft EPS architecture candidates and to study the interactions between individual components within the system.

ACKNOWLEDGMENT

This research is being conducted in the frame of CleanSky JTI Project, a FP7 European Integrated Project - <http://www.cleansky.eu>

REFERENCES

- [1]. J. Weimer, "Electrical power technology for the more electric aircraft," in Conference Proceedings of *IEEE DASC* 1993, vol. 3, pp.445-450, 1993
- [2]. K.J. Karimi, "The role of power electronics in more-electric airplanes (MEA)," presentation at 2006 *IEEE Workshop on Computers in Power Electronics*, July 2006
- [3]. S. N. Mohan, W.P. Robbins and T.M. Underland, "Simulation of Power Electronic and Motion Control Systems- An Overview," *IEEE Proceedings*, August 1994, vol. 82, pp. 1287-1302.
- [4]. **More Open Electrical Technologies (MOET project):** <http://www.moetproject.eu>
- [5]. R. Pena, J. C. Clare, and G. M. Asher, "Doubly Fed Induction Generator using back-to-back PWM Converters and its application to variable-speed wind-energy generation," *IEE Proceedings. on Electric Power Applications*, Vol.143, pp. 380-387, Sept. 1999
- [6]. S. R. Sanders, J. M. Noworolski, X. Z. Liu, and G. C. Verghese, "Generalized averaging method for power conversion circuits," *IEEE Trans.Power Electron.*, vol. 6, pp. 251-259, Apr. 1991.
- [7]. T.Wu, S.V. Bozhko, G.M. Asher and D.W.P. Thomas. "Accelerated functional modeling of aircraft electrical power systems including fault scenarios", in Proceedings of 2009 *IECON IEEE Industrial Electronic Society Conference*, p.2537-2544.
- [8]. T.Wu, S.V. Bozhko, G.M. Asher and D.W.P. Thomas. "A Fast Dynamic Phasor Model of Autotransformer Rectifier Unit for More Electric Aircraft", in Proceedings of 2009 *IECON IEEE Industrial Electronic Society Conference*, p.2531-2536.
- [9]. T.Wu, S.V. Bozhko, G.M. Asher and P.W. Wheeler, "Fast Reduced Functional Models of Electromechanical Actuators for More-Electric Aircraft Power System Study," in Proceedings of 2008 *SAE Power System Conference*, (Paper #2008-01-2859)
- [10]. T.Wu, S.V. Bozhko, G.M. Asher and D.Thomas, "Fast Functional Modelling of the Aircraft Power System including line fault scenarios," in Proceedings of *IEEE 2010 PEMD Conference – Briton*, UK, 2010.

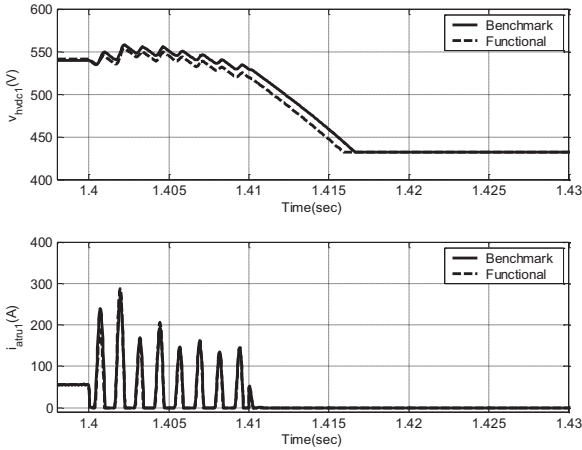


Fig.11. The response of v_{HVDC1} and $i_{dc,ATRU1}$ to a line-to-line fault

Figure 12 shows how the fault effects actuator EMA1 located at the remote HVAC ESS bus. Its dc-link voltage $v_{dc,EMA1}$ falls since the decreased $i_{dc,CRU1}$ is not enough to supply the power demanded by the EMA drive. After the fault clears, the CRU action increases $i_{dc,CRU1}$ to supply additional energy to the dc-link capacitor, and the dc-link voltage $v_{dc,EMA1}$ recovers with the shown transient.

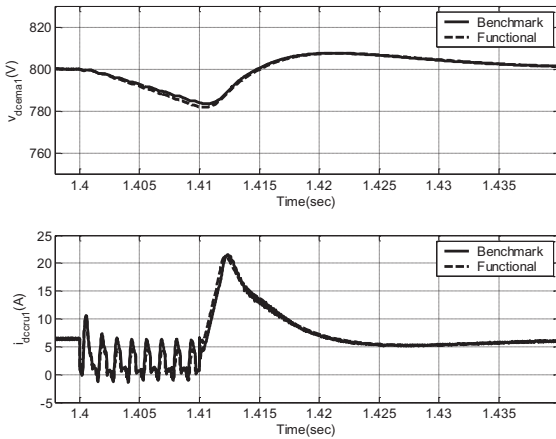


Fig.12. The response of $v_{dc,EMA1}$ and $i_{dc,CRU1}$ to a line-to-line fault

As one can conclude from the figures above, the proposed functional modelling approach allows accurate study of the EPS interactions during fault conditions as well, including a harsh case of unbalanced line-to-line faults. The simulation time taken to simulate 10ms of pre-fault steady-state, then 10ms of faulty regime and 30ms of after-fault transient for EPS to settle is shown in Table 2. The significant improvement in simulation time is confirmed.

TABLE 2 COMPUTATION TIME TAKEN FOR EPS FAULTS SIMULATION

	SG1 loss	HVDC1 fault	L-to-L fault
Functional model	4.26	5.09s	94s
Benchmark model	328s	432s	2892s
Acceleration gained:	77	83	31